Journal of Materials Science: Materials in Electronics (2018) 29:17187–17194
https://doi.org/10.1007/s10854-018-9810-9

Structural, magnetic and magnetocaloric investigation of $La_{0.67}Ba_{0.33}Mn_{1-x}Ni_xO_3$ (x = 0, 0.025 and 0.075) manganite

N. Kharrat[1] · S. Chihaoui[1] · W. Cheikhrouhou-Koubaa[1] · M. Koubaa[1] · A. Cheikhrouhou[1]

Received: 13 June 2018 / Accepted: 2 August 2018 / Published online: 6 August 2018

Abstract
In this paper, we report the structural, magnetic and magnetocaloric properties of Ni-doped $La_{0.67}Ba_{0.33}Mn_{1-x}Ni_xO_3$ (x = 0, 0.025 and 0.075) manganites. Our compounds were synthesized using the sol–gel method. The structural analysis using Rietveld refinement shows that Ni-doped $LaBaMnO_3$ system crystallizes in the rhombohedral symmetry with $R\bar{3}c$ space group. Magnetization measurements versus temperature in a magnetic applied field of 0.05 T reveal that all the compositions exhibit a transition from a ferromagnetic to paramagnetic phase with increasing temperature. A systematic decrease in the transition temperature is clearly observed upon Ni doping and a near room temperature T_C (302 K) is achieved with x = 0.075 composition. The maximum magnetic entropy change $\left(-\Delta S_M^{max}\right)$ in a magnetic field change of 5 T is found to be 2.12, 2.78 and 1.78 J/kg K for x = 0, 0.025 and 0.075, respectively. At this value of magnetic field, large relative cooling power values are obtained in our samples, especially for x = 0.075 (271 J/kg) making it a promising candidate for magnetic refrigeration near room temperature.

1 Introduction

Nowadays, a great attention has been paid to perovskite-type manganese oxides (the so-called manganites) with general formula $RE_{1-x}AE_xMnO_3$ (RE = rare-earth element and AE = alkaline-earth element) owing to their intriguing magnetic properties [1] and large magnetocaloric effect (MCE) [2–4]. The interest of these materials is related to their possible applications in magnetic refrigeration (MR) which is considered to be more energy efficient and environmental friendly compared to traditional gas-compression refrigeration [5–7]. MCE, the base of MR technology, refers to the isothermal magnetic entropy change (accompanied by adiabatic temperature variation) of a magnetic material induced by the application of an external magnetic field. This effect is maximized when the material is near its magnetic ordering temperature (Curie temperature, T_C in the case of ferromagnetic materials) [8, 9]. The research of new materials which exhibit large MCE at low applied fields close to room temperature becomes the main challenge today in order to achieve active magnetic refrigerants working at room temperature. Manganite oxides have been suggested as good candidates for applications in MR technology, since they present some advantageous properties like their extraordinary chemical stability, low cost, easy preparation and high resistivity. Moreover, high magnetic entropy change at low magnetic field changes, wide working temperature ranges and the ability to tailor the magnetic transition temperatures in the vicinity of room temperature by substitution routes indicate that these systems have potentials for MR at various temperatures including room temperature. Phan and Yu [10] have provided an overview of MCEs in manganites oxides and they have explained that their large magnetic entropy could be originated from the strength of double exchange interaction of Mn^{3+}–O–Mn^{4+} and the strong spin–lattice coupling.

The barium-doped lanthanum manganites ($La_{1-x}Ba_xMnO_3$, LBMO) are typical materials that have been less studied compared to the $La_{1-x}Sr_xMnO_3$ (LSMO) and $La_{1-x}Ca_xMnO_3$ (LCMO) compounds. Meanwhile, LBMO systems are of great interest due to their fascinating magnetic properties and considerable MCE [11–15]. Indeed, LaBa-based manganite is one of the interesting exceptions which do not show any signature of antiferromagnetic and charge orders, in contrast to the LaSr- and LaCa- based manganites [12]. In the case of x = 0.33, this compound undergoes a ferromagnetic (FM)-paramagnetic (PM) transition

✉ N. Kharrat
kharrat.noura@gmail.com

[1] LT2S Lab, Digital Research Center of Sfax, Sfax Technopark, Sakiet-Ezzit, B.P. 275, 3021 Sfax, Tunisia

at $T_C = 350$ K and it shows a magnetic entropy change of 1.72 J/kg K under $\mu_0 H = 2T$ around its magnetic ordering temperature, as reported by Xu et al. [16]. However, the T_C of $La_{0.67}Ba_{0.33}MnO_3$ is quite far from room temperature, limiting its applicability in domestic cooling devices. Fortunately, one can easily tune the transition temperature T_C of perovskite manganites towards room temperature by either La-site or Mn-site doping. During recent years, numerous studies have been made on the effects of the replacement of Mn by foreign elements [17–21]. It has been shown that the introduction of other transition metal elements (Fe, Cr, Ti, etc…) in manganites system always affects the magnetic properties, particularly the decreasing of T_C which depends on the nature of doping element. Among these doping elements, nickel (Ni) is of particular interest due to its effects of the Mn-site substitution on the magnetic and magnetocaloric properties [22–24]. It has been observed that Ni doping at Mn site alters the curial Mn^{3+}–O–Mn^{4+} network. In turn, it affects the strength of double-exchange interaction between Mn^{3+} and Mn^{4+} via oxygen and hence causes an additional change in the magnetic properties as well as MCE in doped manganites. In the vast literature on manganites, it is worth noting that there is no published report concerning the effect of Ni content on the magnetocaloric properties of LBMO systems.

In this context, the main objective of our work is to tune the MCE of $La_{0.67}Ba_{0.33}MnO_3$ to near room temperature with Ni substitution. Hence, the present study deals the effect of Ni-doping on the structural, magnetic and magnetocaloric properties of $La_{0.67}Ba_{0.33}Mn_{1-x}Ni_xO_3$ (x = 0, 0.025 and 0.075) compounds synthesized by sol–gel method.

2 Experimental details

Polycrystalline samples $La_{0.67}Ba_{0.33}Mn_{1-x}Ni_xO_3$ (x = 0, 0.025 and 0.075) were prepared by the sol–gel method from La_2O_3, $BaCO_3$, MnO_2 and Ni_2O_3 (99.9% purity) precursors in the appropriate stoichiometric proportions. The precursors were dissolved in nitric acid with continues stirring at 60 °C. Suitable amounts of citric acid and ethylene glycol were added until a completely homogeneous and transparent solution was achieved. The solution was then evaporated at 130 °C, resulting in the formation of a gel. The later was dried at 300 °C and calcined at 600 °C with intermediate grinding to get fine powders. The samples were then pressed into pellets (of about 1 mm thickness under an axial pressure of 4 tons for 2 min) and sintered at 1000 °C for 24 h, crushed, pressed another time and finally heated up to 1100 °C in air for 24 h.

The structure, phase purity and homogeneity were determined by X-ray powder diffraction (XRD) at room temperature using a ''Panalytical X'Pert Pro'' diffractometer with CuK_α radiation ($\lambda = 1.54059$ Å) between 10° and 80° with a step size of 0.02° in 2θ mode. The diffraction data were performed by the Rietveld [25] method using the FULLPROF program [26]. Magnetization measurements versus temperature in the range 50–400 K and versus magnetic applied field up to 5 T were recorded by a vibrating sample magnetometer (VSM) J3590 mini CFM of Cryogenics. MCE results were estimated from the magnetization measurements versus magnetic applied field up to 5 T at several temperatures.

3 Results and discussion

3.1 Structural properties

Figure 1 shows the room temperature X-ray diffraction (XRD) patterns with the fitted curves of the synthesized $La_{0.67}Ba_{0.33}Mn_{1-x}Ni_xO_3$ (x = 0, 0.025 and 0.075) samples. As shown in this figure, XRD patterns prove that all our samples are single phase and can be indexed in the rhombohedral system (Hexagonal setting) with $R\bar{3}c$ space group. Thus, by substitution no apparent structural changes can be identified. Rietveld refinement yields a good fit between the observed and the calculated profiles. The refined structural parameters as well as the goodness of the fit factor (χ^2) are grouped in Table 1. We can see in this table that the unit cell volume decreases with the replacement of partial Mn ions by Ni ions, which confirm the incorporation of Ni in the Mn site. This observation of structural behavior agrees well with those reported in the literature for Ni-doped manganites [22, 27]. This decrease may be due to a smaller ionic radius of Ni^{3+} (0.56 Å) in comparison with that of Mn^{3+} (0.645 Å) [28].

The average crystallite size (D_{SC}) was calculated using Scherrer relation as follows [29]:

$$D_{SC} = \frac{K\lambda}{\beta \cos\theta}, \quad (1)$$

where K = 0.9 is the shape factor, λ is the X-ray wavelength, θ is the diffraction angle and β is the full width at half maximum (FWHM) of the most intense peak. The values of the average crystallite size are given in Table 1.

3.2 Magnetic properties

The magnetization as a function of temperature M (T) curves measured in the field-cooled (FC) mode under an applied magnetic field of 0.05 T for $La_{0.67}Ba_{0.33}Mn_{1-x}Ni_xO_3$ (x = 0, 0.025 and 0.075) samples are depicted in Fig. 2. Our synthesized samples exhibit a paramagnetic (PM) to ferromagnetic (FM) transition with decreasing temperature. The magnetic transition

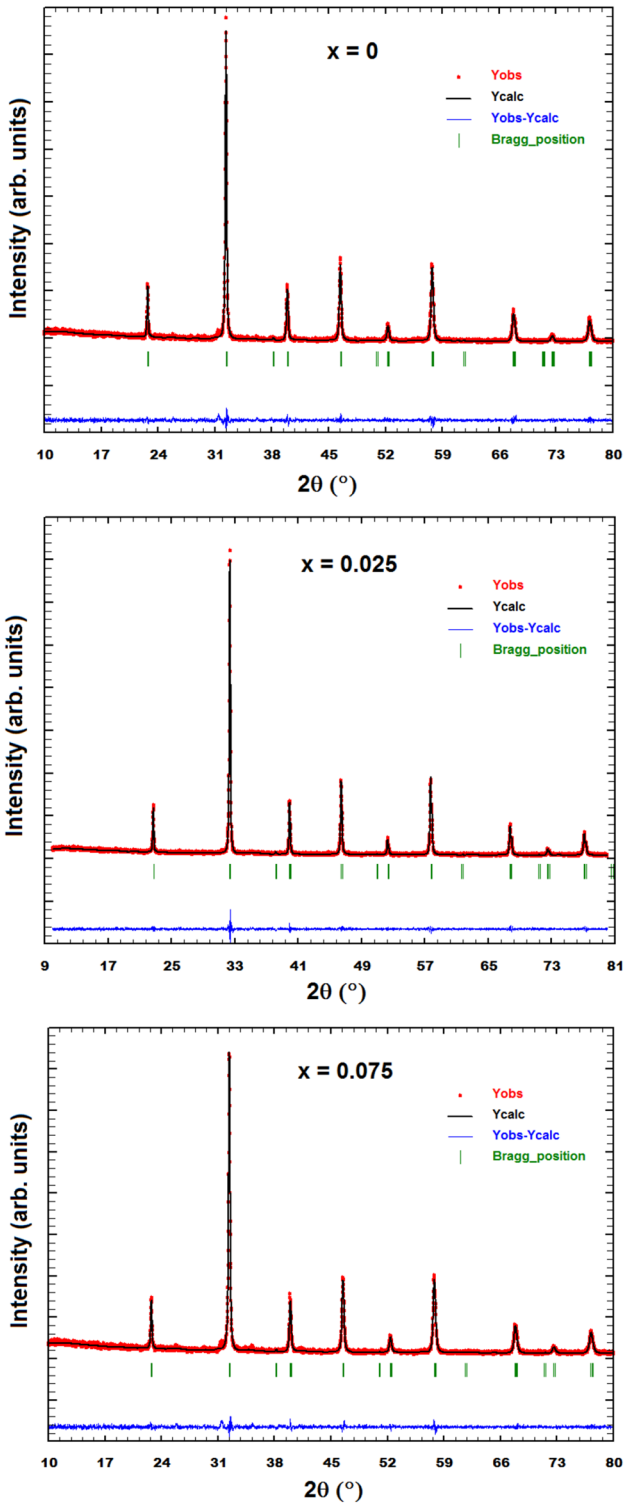

Fig. 1 X-ray diffraction patterns and the corresponding Rietveld refinement for $La_{0.67}Ba_{0.33}Mn_{1-x}Ni_xO_3$ (x = 0, 0.025 and 0.075) compounds at room temperature

temperature T_C, determined from the minimum of the dM/dT curve, shifts to lower temperature with Ni substitution. The obtained Curie temperature values are found to be

Table 1 Refined structural parameters of $La_{0.67}Ba_{0.33}Mn_{1-x}Ni_xO_3$ (x = 0, 0.025 and 0.075) compounds and crystallite size estimated from the Scherrer method

x	0	0.025	0.075
Space group	$R\bar{3}c$	$R\bar{3}c$	$R\bar{3}c$
a = b (Å)	5.5252	5.5259	5.5212
c (Å)	13.5520	13.5390	13.5350
V (Å^3)	358.2861	358.0331	357.3187
$\langle\theta_{Mn/Ni-O-Mn/Ni}\rangle$ (°)	164.09 (2)	163.53 (2)	162.88 (3)
$\langle d_{Mn/Ni-O}\rangle$ (Å)	1.9733 (2)	1.97421 (16)	1.9746 (3)
χ^2	1.31	1.25	1.36
D_{SC} (nm)	52	71	43

336, 328 and 302 K for x = 0, 0.025 and 0.075, respectively. The trend of reduction in T_C is consistent with the results reported in [22–24] for Ni-doped manganites. The substitution of Ni ions into the Mn site disturbs the Mn^{3+}–O–Mn^{4+} chains, which leads to a change in the Mn^{3+}/Mn^{4+} ratio [30]. As a consequence of this variation, the double exchange (DE) interaction, which is the origin of the ferromagnetism in the manganites is weakened [31], and therefore the T_C will decrease. Also, the partial substitution of Mn^{3+} by Ni^{3+} ions generates new antiferromagnetic (AFM) bonds between Ni and Mn ions, which are non-DE interactions and therefore promote AFM coupling. The promotion of AFM coupling then weakens the DE and lowers the T_C. Moreover, the decrease in T_C is mainly explained by the decrease of $\langle\theta_{Mn/Ni-O-Mn/Ni}\rangle$ bond angle and the increase of $\langle d_{Mn/Ni-O}\rangle$ bond length as the Ni content increases (Table 1). Both effects lead to the decrease of the bandwidth W and the mobility of e_g electrons. For ABO_3-type perovskites, the bandwidth W can be expressed empirically by [32]:

$$W \approx \frac{\cos\left[1/2\left(\pi - \langle\theta_{Mn/Ni-O-Mn/Ni}\rangle\right)\right]}{\left(d_{Mn/Ni-O}\right)^{3.5}}. \quad (2)$$

The calculated values of W are 0.0917, 0.0915 and 0.0914 for x = 0, 0.025 and 0.075, respectively. The observed decrease, induced by the Ni doping, reduces the overlap between the 3d orbital of the Mn ions at B-site and the 2p orbital of the O anion, which in turn weakens the DE coupling of Mn^{3+}–O–Mn^{4+}, and hence reduces the FM coupling between neighboring manganese, resulting in a reduction of T_C as well. Similar behaviors were previously reported in $La_{0.67}Ba_{0.33}Mn_{1-x}Cr_xO_3$ [33] and $La_{0.7}Sr_{0.3}Mn_{0.9}M_{0.1}O_3$ (M = Cr, Sn and Ti) [21]. Interestingly, our T_C values span the room temperature range, which is beneficial for magnetic refrigeration at room temperature.

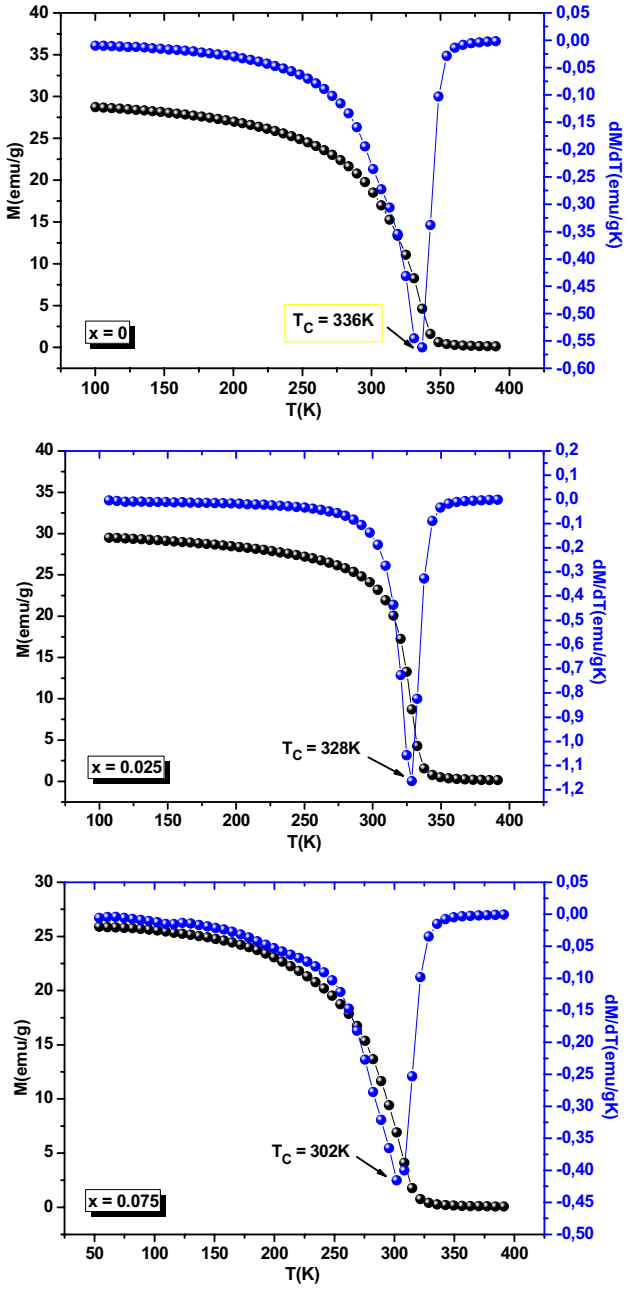

Fig. 2 Variation of the magnetization versus temperature M (T) and the dM/dT curves as a function of temperature measured at $\mu_0 H = 0.05$ T

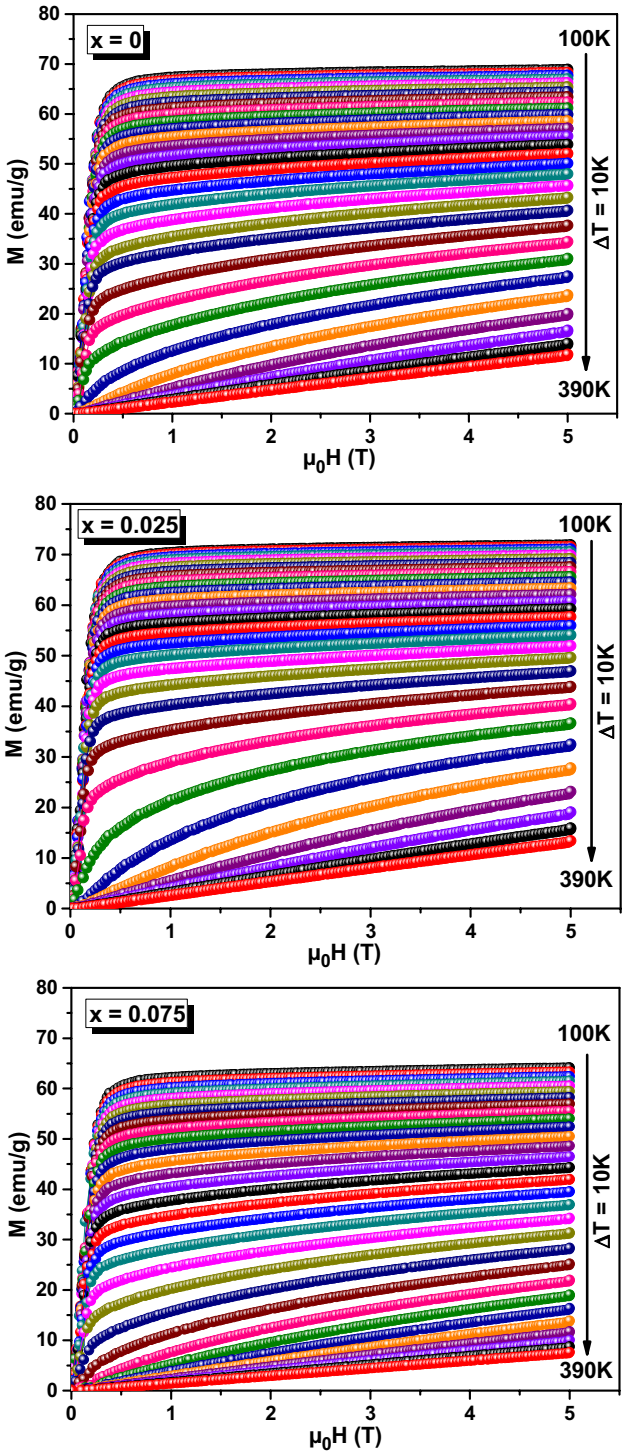

Fig. 3 Isothermal magnetization curves for $La_{0.67}Ba_{0.33}Mn_{1-x}Ni_xO_3$ (x = 0, 0.025 and 0.075) compounds

In order to confirm the ferromagnetic behavior at low temperatures of our samples we measure the isothermal magnetization versus magnetic applied field $\mu_0 H$ up to 5 T at several temperatures, which is plotted in Fig. 3. For all the studied samples, the magnetization below T_C increases quickly at low magnetic fields and tend to saturation above 1 T, corresponding to ferromagnetic state.

The Arrott plots M^2 versus $\mu_0 H$ are used to clarify the nature of the FM–PM phase transition based on the measured data of the M ($\mu_0 H$) isotherms [34]. The order of the magnetic transition can be determined from the slope of Arrott plot according to the criterion proposed by Banerjee

[35], i.e., a negative slope corresponds to first order magnetic transition while a positive slope corresponds to second order one. The Arrott plots reported in Fig. 4 gives a positive slope for all the temperatures. This implies that our samples undergo a second-order magnetic phase transition.

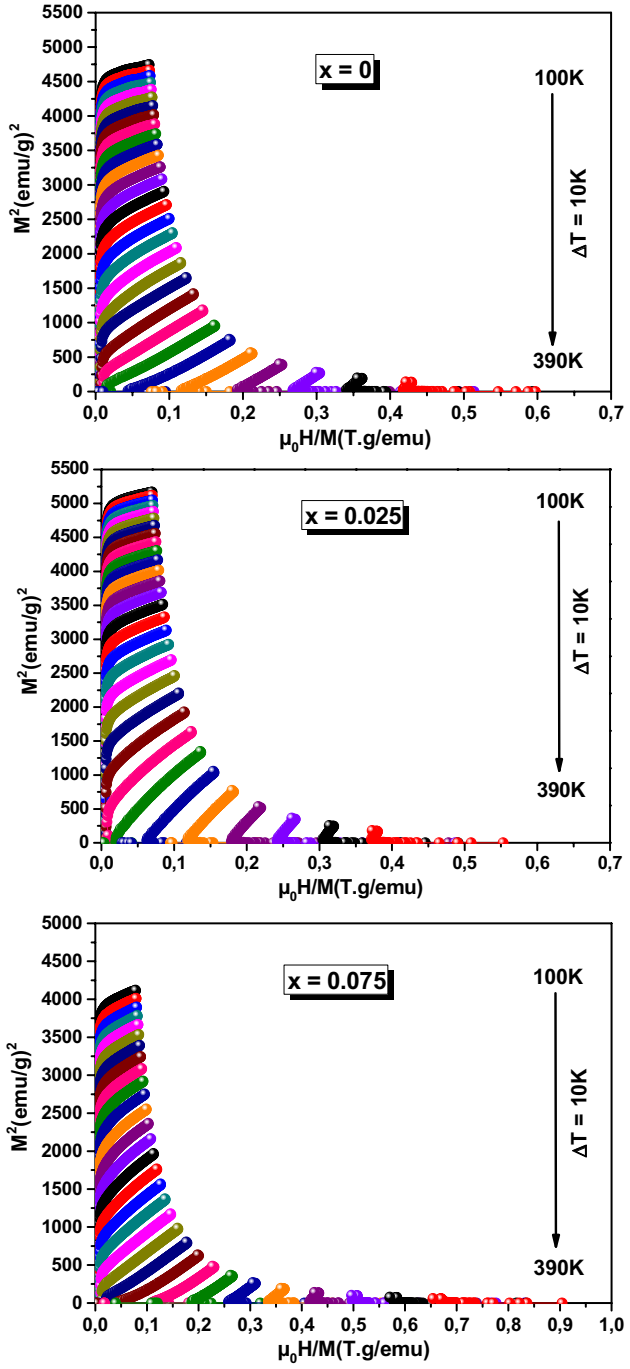

Fig. 4 Arrott plots (M^2 as a function of $\mu_0 H/M$) for $La_{0.67}Ba_{0.33}Mn_{1-x}Ni_xO_3$ (x = 0, 0.025 and 0.075) compounds

3.3 Magnetocaloric properties

In order to study the MCE in the investigated materials, the changes of magnetic entropy upon application of magnetic fields can be calculated using the thermodynamic Maxwell's relation given by the following equation [10, 36]:

$$\Delta S_M(T, \mu_0 H) = S_M(T, \mu_0 H) - S_M(T, 0) = \int_0^{\mu_0 H} \left(\frac{\partial M(T, \mu_0 H)}{\partial T} \right)_{\mu_0 H} \mu_0 dH \,. \quad (3)$$

For magnetization measurements performed at discrete fields and temperature intervals, the magnetic entropy change defined in Eq. (3) can be approximated as [10, 36]:

$$\Delta S_M(T, \mu_0 H) = \sum_i \frac{M_{i+1}(T_{i+1}, \mu_0 H) - M_i(T_i, \mu_0 H)}{T_{i+1} - T_i} \mu_0 \Delta H, \quad (4)$$

where M_i and M_{i+1} are the experimental values of magnetization measured at temperatures T_i and T_{i+1}, respectively, under an applied magnetic field $\mu_0 H$.

From the isothermal magnetization measurements, one can calculate the magnetic entropy change associated with magnetic field variation using Eq. (4). The correspondingly calculated $-\Delta S_M(T, \Delta H)$ curves are plotted in Fig. 5. This figure shows an increase in $-\Delta S_M$ with increasing $\mu_0 H$ from 1 to 5 T for each composition. The $-\Delta S_M$ is found to be positive in the entire temperature range for all magnetic fields, which confirms the ferromagnetic character. It is obviously that the magnetic entropy change originates from the considerable change of magnetization in the vicinity of T_C. As expected, ΔS_M alternates with temperature and exhibits a peak at a temperature near its PM–FM transition temperature at all applied fields. Furthermore, the maximum of magnetic entropy changes, $-\Delta S_M^{max}$, shifts towards lower temperatures when the Ni content increases, following the same trend of T_C (Fig. 2) that is tuned towards room temperature by the substitution. The downward shift of $-\Delta S_M^{max}$ with Ni doping provides the opportunity to fabricate compounds useful for magnetic refrigeration around room temperature. For $\mu_0 H = 5$ T, $-\Delta S_M^{max}$ is found to be 2.12, 2.78 and 1.78 J/kg K, for x = 0, 0.025 and 0.075 samples, respectively.

The evaluation of the cooling efficiency of a magnetocaloric material passes through the so-called relative cooling power (RCP) [10, 37] corresponding to the amount of heat transferred between the cold and the hot skins in the ideal refrigeration cycle. RCP depends on both the maximum value of the magnetic entropy change $\left(-\Delta S_M^{max}\right)$ and the full-width at half-maximum δT_{FWHM} of the magnetic entropy change curve. It is given by:

$$RCP = -\Delta S_M^{max}(T, \mu_0 H) \times \delta T_{FWHM} \quad (5)$$

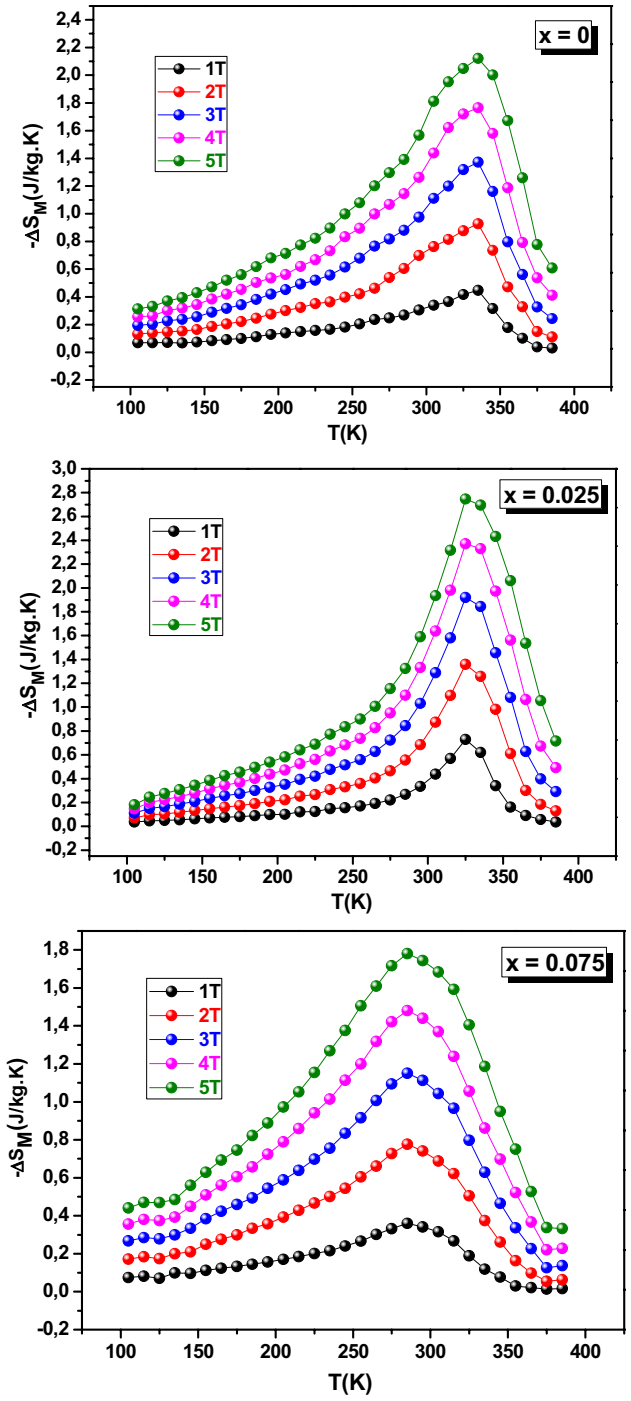

Fig. 5 Temperature dependence of the magnetic entropy change at several magnetic fields for $La_{0.67}Ba_{0.33}Mn_{1-x}Ni_xO_3$ (x = 0, 0.025 and 0.075) samples

The different values of RCP of our samples under a magnetic field varying from 1 to 5 T at T_C are shown in Fig. 6. It is clearly observed that RCP values increase linearly with increasing the applied magnetic field, which is due to the effect of spin coupling that is less important when the applied magnetic field is higher. A comparison between the

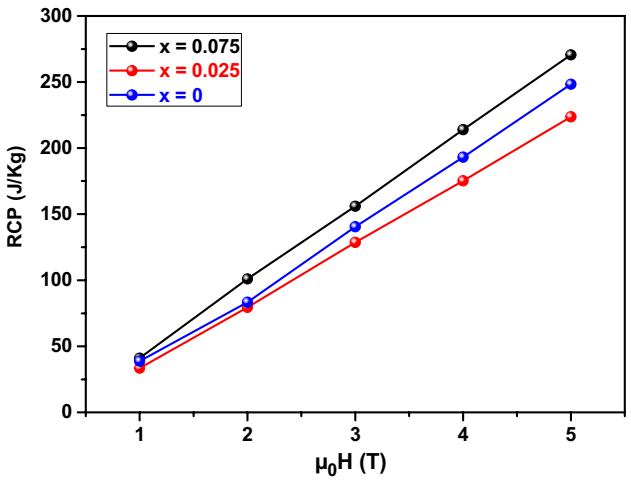

Fig. 6 The magnetic field dependence of RCP for $La_{0.67}Ba_{0.33}Mn_{1-x}Ni_xO_3$ (x = 0, 0.025 and 0.075) samples

RCP values corresponding to a magnetic field of 5 T for our studied systems and other magnetocaloric materials is also presented in Table 2. As can be seen from this table, our RCP values are larger than those obtained for other perovskite manganites around room temperature [22, 38–43]. Moreover, our RCP values for x = 0, 0.025 and 0.075 compounds are respectively about 60%, 54% and 66% of that of the prototype magnetic refrigerant material Gd [7] for the same field change. Among the samples, the x = 0.075 composition shows the highest RCP of 271 J/kg under 5 T around room temperature. In magnetic refrigeration technology, a promising material for magnetic refrigeration application should have higher RCP and the value of T_C should be close to room temperature. Therefore we can deduce that $La_{0.67}Ba_{0.33}Mn_{0.925}Ni_{0.075}O_3$ material possesses appropriate properties for a good candidate as magnetic cooling at ambient temperature.

4 Conclusion

$La_{0.67}Ba_{0.33}Mn_{1-x}Ni_xO_3$ (x = 0, 0.025 and 0.075) manganites were synthesized via the sol–gel method and their structural, magnetic, and magnetocaloric properties were investigated. All our samples crystallize in the rhombohedral structure with the $R\bar{3}c$ space group. Magnetic measurements show that all compounds present a second order PM-FM phase transition with a decrease in Curie temperature T_C, probably due to the decrease of the ferromagnetic double exchange (DE) interactions. For $La_{0.67}Ba_{0.33}Mn_{0.925}Ni_{0.075}O_3$ composition, the maximum value of the magnetic entropy change is found to be 1.78 J/kg K and the relative cooling power is about 271 J/kg under 5 T at 302 K. The achieved results suggest

Table 2 Experimental values of T_C, magnetic entropy change $-\Delta S_M^{max}$ and relative cooling power (RCP) for $La_{0.67}Ba_{0.33}Mn_{1-x}Ni_xO_3$ (x = 0, 0.025 and 0.075) compounds in comparison with those of several magnetocaloric materials taken from the literature

Compositions	T_C (K)	$\mu_0 H$ (T)	$-\Delta S_M^{max}$ (J/kg K)	RCP (J/kg)	References
$La_{0.67}Sr_{0.33}Mn_{0.9}Ni_{0.1}O_3$	290	5	3	132	[22]
$La_{0.57}Nd_{0.1}Sr_{0.23}MnO_3$	339	5	4.42	186	[38]
$La_{0.67}Ba_{0.33}MnO_3$	292	5	1.48	161	[39]
$La_{0.57}Nd_{0.1}Sr_{0.33}Mn_{0.95}Sn_{0.05}O_3$	281	5	2.8	51	[40]
$La_{0.6}Nd_{0.1}(CaSr)_{0.3}Mn_{0.9}V_{0.1}O_3$	298	5	4.266	205.35	[41]
$La_{0.7}Sr_{0.3}MnO_3$	319	5	1.63	178	[42]
$La_{0.69}Dy_{0.01}Sr_{0.3}MnO_3$	315	5	1.21	114	[42]
$La_{0.6}Ca_{0.2}Ba_{0.2}MnO_3$	302	5	2.40	176	[43]
Gd	294	5	10.2	410	[7]
$La_{0.67}Ba_{0.33}MnO_3$	336	5	2.12	248	This work
$La_{0.67}Ba_{0.33}Mn_{0.975}Ni_{0.025}O_3$	328	5	2.78	224	This work
$La_{0.67}Ba_{0.33}Mn_{0.925}Ni_{0.075}O_3$	302	5	1.78	271	This work

that the $La_{0.67}Ba_{0.33}Mn_{0.925}Ni_{0.075}O_3$ can thus be used as an active magnetic refrigerator working at room temperature.

Acknowledgements This study was supported by the Tunisian Ministry of Higher Education and Scientific Research.

References

1. C. Martin, A. Maignan, M. Hervieu, B. Raveau, Magnetic phase diagrams of $L_{1-x}A_xMnO_3$ manganites, L = Pr, Sm; A = Ca, Sr… Phys. Rev. B **60**, 12191 (1999)
2. Y. Sun, W. Tong, Y. Zhang, Large magnetic entropy change above 300 K in $La_{0.70}Ca_{0.20}Sr_{0.10}MnO_3$. J. Magn. Magn. Mater. **232**, 205 (2001)
3. G.C. Lin, Q. Wie, J.X. Zhang, Direct measurement of the magnetocaloric effect in $La_{0.67}Ca_{0.33}MnO_3$. J. Magn. Magn. Mater. **300**, 392 (2006)
4. Y. Regaieg, L. Sicard, J. Monnier, M. Koubaa, S. Ammar-Merah, A. Cheikhrouhou, Magnetic and magnetocaloric properties of $La_{0.85}(Na_{1-x}K_x)_{0.15}MnO_3$ ceramics produced by reactive spark plasma sintering. J. Appl. Phys. **115**, 17A917 (2014)
5. O. Tegus, E. Brück, K.H.J. Buschow, F.R. de Boer, Transition-metal-based magnetic refrigerants for room-temperature applications. Nature **415**, 150 (2002)
6. E. Brück, Developments in magnetocaloric refrigeration. J. Phys. D **38**, R381 (2005)
7. K.A. Gschneidner Jr., V.K. Pecharsky, A.O. Tsokol, Recent developments in magnetocaloric materials. Rep. Prog. Phys. **68**, 1479 (2005)
8. A.M. Tishin, I. Spichkin, *The Magnetocaloric Effect and its Applications* (Institute of Physics Publishing, Bristol, 2003)
9. V. Franco, J.S. Blazquez, B. Ingale, A. Conde, The magnetocaloric effect and magnetic refrigeration near room temperature: materials and models. Annu. Rev. Mater. Res. **42**, 305 (2012)
10. M.H. Phan, S.C. Yu, Review of the magnetocaloric effect in manganite materials. J. Magn. Magn. Mater. **308**, 325 (2007)
11. A. Barnabé, F. Millange, A. Maignan, M. Hervieu, B. Raveau, G. Van Tendeloo, P. Laffez, Barium-based manganites $Ln_{1-x}Ba_xMnO_3$ with Ln = {Pr, La}: phase transitions and magnetoresistance properties. Chem. Mater. **10**, 252 (1998)
12. H.L. Ju, Y.S. Nam, J.E. Lee, H.S. Shin, Anomalous magnetic properties and magnetic phase diagram of $La_{1-x}Ba_xMnO_3$. J. Magn. Magn. Mater. **219**, 1 (2000)
13. C. Osthover, P. Grtinberg, R.R. Arons, Magnetic properties of doped $\{La_{0.67}Ba_{0.33}\}$ $\{Mn_{1-y}A_y\}O_3$, A = Fe, Cr. J. Magn. Magn. Mater. **177–181**, 854–855 (1998)
14. A.A.E.M. Mohamed, B.Hernando, The expected low field magnetocaloric effect of $La_{0.7}Ba_{0.3}MnO_3$ manganite at room temperature. Phys. Lett. A **380**, 1763 (2016)
15. S. Ghodhbane, A. Dhahri, N. Dhahri, E.K. Hlil, J. Dhahri, Structural, magnetic and magnetocaloric properties of $La_{0.8}Ba_{0.2}Mn_{1-x}Fe_xO_3$ compounds with $0 \le x \le 0.1$. J. Alloys Compd. **550**, 358 (2013)
16. Y. Xu, M. Meter, P. Das, M.R. Kobischka, U. Hartmann, Perovskite manganites: potential materials for magnetic cooling at or near room temperature. Cryst. Eng. **5**, 383 (2002)
17. S.K. Barik, C. Krishnamoorthi, R. Mahendiran, Effect of Fe substitution on magnetocaloric effect in $La_{0.7}Sr_{0.3}Mn_{1-x}Fe_xO_3$ ($0.05 \le x \le 0.20$). J. Magn. Magn. Mater. **323**, 1015 (2011)
18. A. Mleiki, S. Othmani, W. Cheikhrouhou-Koubaa, A. Cheikhrouhou, E.K. Hlil, Enhanced relative cooling power in Ga-doped $La_{0.7}(Sr,Ca)_{0.3}MnO_3$ with ferromagnetic-like canted state. RSC Adv. **6**, 54299 (2016)
19. R. Bellouz, M. Oumezzine, E.K. Hlil, E. Dhahri, Effect of Cr substitution on magnetic and magnetic entropy change of $La_{0.65}Eu_{0.05}Sr_{0.3}Mn_{1-x}Cr_xO_3$ ($0.05 \le x \le 0.15$) rhombohedral nanocrystalline near room temperature. J. Magn. Magn. Mater. **375**, 136 (2015)
20. F. Ben Jemaa, S. Mahmood, M. Ellouze, E.K. Hlil, E. Halouani, Structural, magnetic, and magnetocaloric studies of $La_{0.67}Ba_{0.22}Sr_{0.11}Mn_{1-x}Co_xO_3$ manganites. J. Mater. Sci. **50**, 620 (2015)
21. B. Arayedh, S. Kallel, N. Kallel, O. Peña, Influence of non-magnetic and magnetic ions on the MagnetoCaloric properties of $La_{0.7}Sr_{0.3}Mn_{0.9}M_{0.1}O_3$ doped in the Mn sites by M = Cr, Sn, Ti. J. Magn. Magn. Mater. **361**, 68 (2014)
22. C.P. Reshmi, S. Savitha Pillai, K.G. Suresh, M.R. Varma, Room temperature magnetocaloric properties of Ni substituted $La_{0.67}Sr_{0.33}MnO_3$. Solid State Sci. **19**, 130 (2013)
23. T.-L. Phan, Q.T. Tran, P.Q. Thanh, P.D.H. Yen, T.D. Thanh, S.C. Yu, Critical behavior of $La_{0.7}Ca_{0.3}Mn_{1-x}Ni_xO_3$ manganites exhibiting the crossover of first- and second-order phase transitions. Solid State Commun. **184**, 40 (2014)
24. S.H. Hua, P.Y. Zhang, H.F. Yang, S.Y. Zhang, H.L. Ge, The magnetic and magnetocaloric properties of the perovskite $La_{0.7}Ca_{0.3}Mn_{1-x}Ni_xO_3$. J. Magn. **18**, 34 (2013)
25. H.M. Rietveld, A profile refinement method for nuclear and magnetic structures. J. Appl. Cryst. **2**, 65 (1969)

26. T. Roisnel, J. Rodriguez-Carvajal, C. Program FULLPROF, LLB-LCSIM (2003)
27. X.S. Ge, Z.Z. Li, W.H. Qi, D.H. Ji, G.D. Tang, L.L. Ding, J.J. Qian, Y.N. Du, Magnetic and electrical transport properties of perovskite manganites $Pr_{0.6}Sr_{0.4}M_xMn_{1-x}O_3$ (M = Fe, Co, Ni). AIP Adv. **7**, 125002 (2017)
28. R.D. Shannon, Revised effective ionic radii and systematic studies of interatomic distances in halides and chalcogenides. Acta Crystallogr. A **32**, 751 (1976)
29. A. Taylor, *X-ray Metallography* (Wiley, New York, 1961)
30. Y. Bitla, S.N. Kaul, L.F. Barquin, J. Gutierrez, J.M. Barandiaran, A. Pena, Observation of isotropic-dipolar to isotropic-Heisenberg crossover in Co- and Ni-substituted manganites. New J. Phys. **12**, 093039 (2010)
31. C. Zener, Interaction between the d-shells in the transition metals. II. Ferromagnetic compounds of manganese with perovskite structure. Phys. Rev. **82**, 403 (1951)
32. M. Medarde, J. Mesot, P. Lacorre, S. Rosenkranz, P. Fischer, K. Gobrecht, High-pressure neutron-diffraction study of the metallization process in $PrNiO_3$. Phys. Rev. B **52**, 9248 (1995)
33. M. Oumezzine, O. Peña, S. Kallel, T. Guizouarn, M. Oumezzine, Structural studies and magnetic and transport properties of Cr-substituted $La_{0.67}Ba_{0.33}Mn_{1-x}Cr_xO_3$ ($0 \le x \le 0.15$) perovskites. J. Alloys Compd. **533**, 33 (2012)
34. A. Arrott, Criterion for ferromagnetism from observations of magnetic isotherms. Phys. Rev. **108**, 1394 (1957)
35. S.K. Banerjee, On a generalized approach to first and second order magnetic transitions. Phys. Lett. **12**, 16 (1964)
36. X. Bohigas, J. Tejada, M.L. Marinez-Sarrion, S. Tripp, R. Black, Magnetic and calorimetric measurements on the magnetocaloric effect in $La_{0.6}Ca_{0.4}MnO_3$. J. Magn. Magn. Mater. **208**, 85 (2000)
37. K.A. Gschneidner Jr., V.K. Pecharsky, Magnetocaloric materials. Annu. Rev. Mater. Sci. **30**, 387 (2000)
38. S. Mnefgui, A. Dhahri, N. Dhahri, El.K. Hlil, J. Dhahri, The effect deficient of strontium on structural, magnetic and magnetocaloric properties of $La_{0.57}Nd_{0.1}Sr_{0.33-x}MnO_3$ (x = 0.1 and 0.15) manganite. J. Magn. Magn. Mater. **340**, 91 (2013)
39. D.T. Morelli, A.M. Mance, J.V. Mantese, A.L. Micheli, Magnetocaloric properties of doped lanthanum manganite films. J. Appl. Phys. **79**, 373 (1996)
40. E. Tka, K. Cherif, J. Dhahri, Evolution of structural, magnetic and magnetocaloric propertiesin Sn-doped manganites $La_{0.57}Nd_{0.1}Sr_{0.33}Mn_{1-x}Sn_xO_3$ (x = 0.05–0.3). Appl. Phys. A **116**, 1181 (2014)
41. A. Dhahri, F.I.H. Rhouma, S. Mnefgui, J. Dhahri, E.K. Hlil, Room temperature critical behavior and magnetocaloric properties of $La_{0.6}Nd_{0.1}(CaSr)_{0.3}Mn_{0.9}V_{0.1}O_3$. Ceram. Int. **40**, 459 (2014)
42. I. Sfifir, A. Ezaami, W. Cheikhrouhou-Koubaa, A. Cheikhrouhou, Structural, magnetic and magnetocaloric properties in $La_{0.7-x}Dy_xSr_{0.3}MnO_3$ manganites (x = 0.00, 0.01 and 0.03). J. Alloys Comp. **696**, 760 (2017)
43. I. Sfifir, H. Ben Khlifa, W. Cheikhrouhou-Koubaa, M. Koubaa, A. Cheikhrouhou, Vacancy effect in both calcium and barium on the physical properties of $La_{0.6}Ca_{0.2}Ba_{0.2}MnO_3$ polycrystalline manganite. J. Alloys Comp. **693**, 782 (2016)